Pergamon

Tetrahedron: *Asymmetry* 12 (2001) 3125–3137

TETRAHEDRON: *ASYMMETRY*

# Induced chirality upon crocetin binding to human serum albumin: origin and nature

Ferenc Zsila,* Zsolt Bikádi and Miklós Simonyi

*Department of Molecular Pharmacology, Institute of Chemistry, Chemical Research Center, Budapest, POB 17, 1525, Hungary*

Received 26 October 2001; accepted 5 December 2001

**Abstract**—Binding to human serum albumin (HSA) of the natural, achiral carotenoid crocetin, having hypocholesterolemic and antitumour effects, was investigated in detail by circular dichroism (CD) and absorption spectroscopy. It has been shown that in the visible absorption region the crocetin–HSA complex exhibits a well-defined induced circular dichroic spectrum with two major bands of opposite sign, proving excitonic interaction between carotenoids bound in a left-handed chiral arrangement on the albumin molecule. In the course of CD titration experiments, palmitic acid gradually decreased the exciton band intensities indicating that crocetin and palmitic acid have common binding sites on HSA. To investigate potential sources of the intermolecular excitonic interaction, molecular modeling studies were performed fitting crocetin molecules to the long-chain fatty acid binding sites of HSA, determined recently by X-ray crystallographic measurements. The results suggest that binding of crocetin to domain III of the albumin might be responsible for the observed intermolecular exciton coupling. Crocetin binding was accompanied by a significant red shift in the visible absorption spectrum which has showed no excitonic contribution but rather indicates the higher polarizability of the protein environment. 

## 1. Introduction

*Crocus sativus* L., commonly known as saffron, is used in folk medicine for various purposes.[1] Modern pharmacological studies have demonstrated that saffron extracts have anti-tumor and hypolipidaemic effects.[2] Among the constituents of saffron extract, crocetin (8,8′-diapocarotene-8,8′-dioic acid),[3] is mainly responsible for these pharmacological activities (Fig. 1). Crocetin was shown to be effective against malignant cells in vitro[4,5] and in vivo[6] exhibiting dose-dependent inhibitory and cytotoxic effects. Also, crocetin has been suggested to enhance the diffusion of $O_2$ through plasma increasing oxygen available to the capillary endothelial cells.[7–9] In addition, several studies have indicated that experimental animal atherosclerosis can be reduced by crocetin treatment[10–12] and that these effects can be related with crocetin binding to plasma proteins.[13]

Human serum albumin (HSA), the most abundant serum protein, is a single-chain 66 kDa protein, which is largely helical and contains 585 amino acids with known sequences.[14,15] The three-dimensional structure of HSA was determined through X-ray crystallographic measurements.[16,17] It consists of three structurally homologous domains (I–III) organized into a heart shape. Albumin binds a variety of substrates, including numerous *endo*- and exogenous hydrophobic molecular species e.g. fatty acids, hormones and several therapeutic drugs.[14,15,18] The distribution, free concentration and the metabolism of various drugs can be significantly altered as a result of their binding to HSA. One of the most important functions of albumin is to bind and carry strongly hydrophobic fatty acids.[19,20] Long-chain fatty acids (e.g. palmitic and stearic acid) have high affinity to albumin and their multiple binding sites have been the subject of several biochemical investigations.[21–24]

Multiple association constants for palmitic acid to HSA were found to be 14.5, 13.0, 7.1, 1.2, 0.8 and $0.3\times10^7$ $M^{-1}$.[24] Recently, X-ray crystallographic studies performed on HSA identified several binding sites occupied by medium-chain and long-chain fatty acids.[25–27] For the latter ones, the primary binding sites were suggested to be located in domains I and III, respectively.

* Corresponding author. Fax: (361) 325-7750; e-mail: zsferi@chemres.hu

0957-4166/01/$ - see front matter 
PII: S0957-4166(01)00552-3

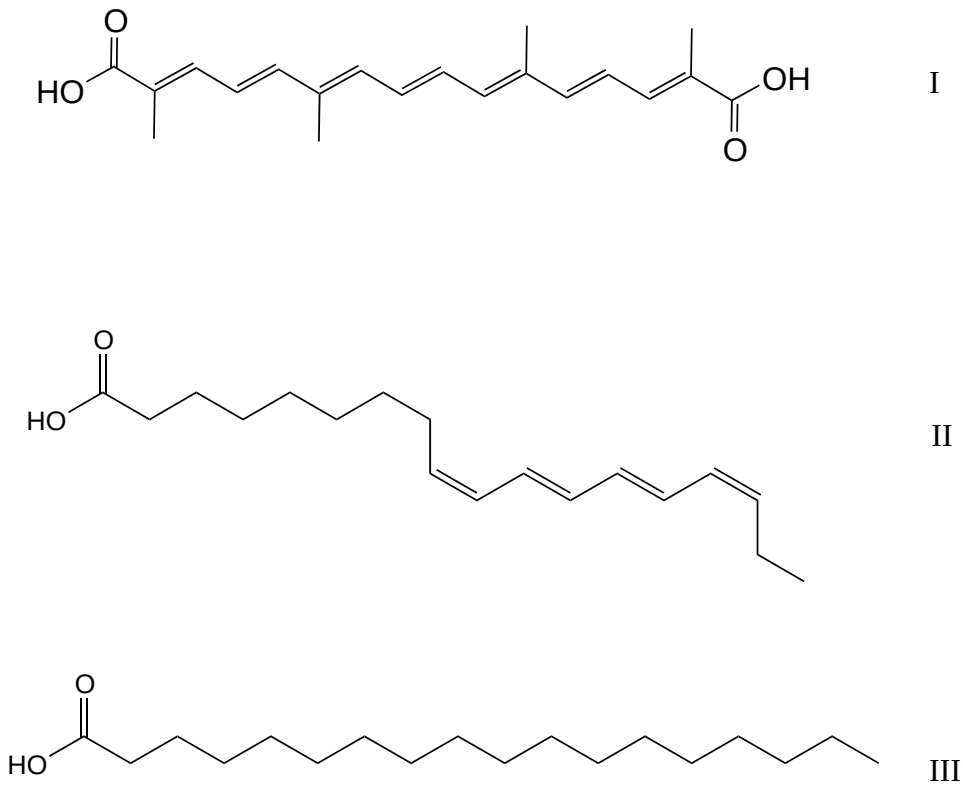


**Figure 1.** Chemical structures of crocetin (8,8′-diapocarotene-8,8′-dioic acid), *cis*-parinaric acid (9,11,13,15-*cis*,*trans*,*trans*,*cis*-octadecatetraenoic acid) and palmitic acid (hexadecanoic acid).

*cis*-Parinaric acid, an 18-carbon conjugated polyene fatty acid (Fig. 1), was used as a probe for lipid–protein interactions.[28,29] Titration experiments showed that defatted bovine (BSA) and HSAs bind 5 and 6 mol parinaric acids with binding constants of $\sim 10^6$ to $10^8$ $M^{-1}$.[29,30] Added quantities of palmitic acid decreased the binding capacity of parinaric acid on BSA. As has been observed, vibronically coupled, negative–positive Cotton effects (CE) appeared upon binding of parinaric acid to BSA and HSA[28,29,31] that have been attributed to an excitonic interaction among two ligands bound in domain III, close to each other.[31]

It is known from the work of Miller et al. that crocetin and palmitic acid have common binding sites on human and bovine serum albumins.[13] These authors utilized absorption and fluorescence spectroscopy techniques to characterize the crocetin–albumin interaction. They found a red shift in the crocetin visible absorption spectrum and reduced tryptophan fluorescence upon albumin binding. For the first crocetin binding site of HSA, the affinity binding constant is $4\times10^6$ $M^{-1}$. Stimulated by these findings, we applied circular dichroism (CD) spectroscopy, an essential tool for probing chirality, to further investigate this notable carotenoid–protein interaction. After finding a strong and very characteristic induced excitonic CD couplet an attempt was made by the aid of molecular modeling studies to correlate it with the stereochemical properties of the known fatty-acid binding sites of HSA.

## 2. Results

The most characteristic feature of the carotenoid structure is the long system of alternating double and single bonds that forms the central part of the molecule. This constitutes a conjugated system in which the π-electrons are effectively delocalized over the entire length of the polyene chain. This feature is responsible for the molecular shape, chemical reactivity and light-absorbing properties, and hence the color of carotenoids. The structure of crocetin features a linear, symmetrical planar polyene chain[32] composed of alternating carbon–carbon single and double bonds (Fig. 1). Similarly to other carotenoids, its hydrophobic character is dominant in spite of the end-chain carboxyl groups. As a consequence, in aqueous solution crocetin tends to form aggregates accompanied with profound changes in the absorption spectrum.[13] At basic pH, however, the ionized carboxyl groups significantly increase the water solubility allowing a true solution to be prepared. Therefore, crocetin was dissolved in a 0.2 M borate buffer (pH 8.5) at a concentration of 10 μM. Fig. 2 displays the crocetin ultraviolet–visible (UV–vis) absorption spectrum between 205 and 550 nm. The origin of the intense absorption band in the visible region is assigned to the electronically allowed but magnetically forbidden singlet–singlet $^1A_g \rightarrow {}^1B_u$ transition of the π electrons due to the $C_{2h}$ symmetry of the conjugated polyene chain, and the direction of the transition moment is parallel to the long molecular axis.[33] The main absorption band carries characteristic

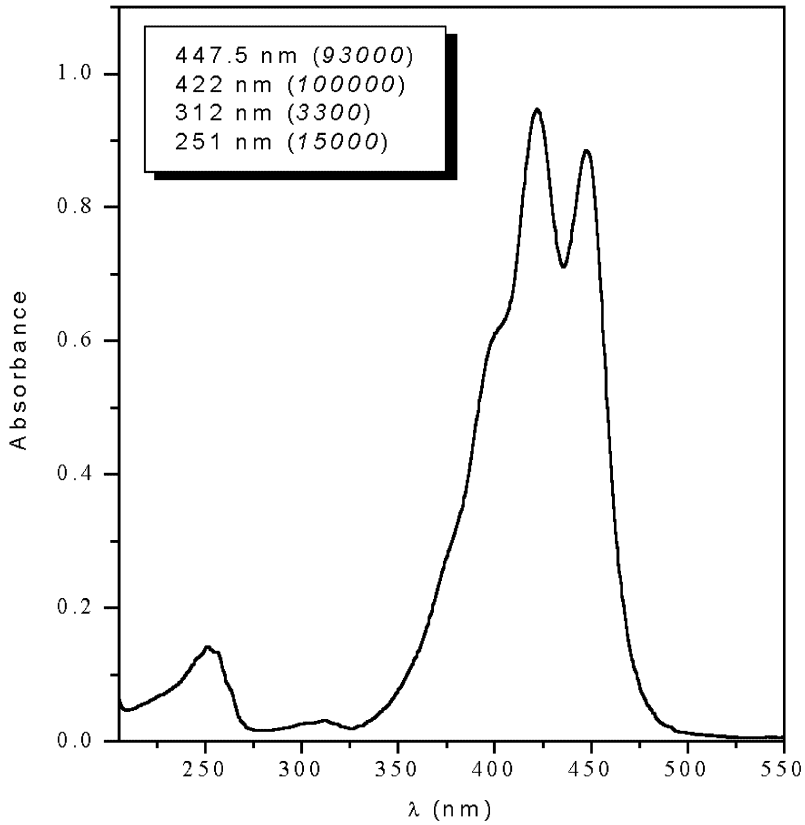


**Figure 2.** UV–vis absorption spectrum of crocetin at room temperature in borate buffer, pH 8.5. Concentration is $10^{-5}$ M, optical path length is 1 cm. Inset shows the peak positions and the molar extinction coefficients in $M^{-1}$ $cm^{-1}$.

vibrational fine structure assigned mainly to the C=C stretching vibration. According to this, the progression is built up by 1550, 1556 and 1557 $cm^{-1}$ vibrational series obtained from the second derivative spectrum (not shown). The weak, high energy band at 312 nm corresponds to a *cis*-isomer of the crocetin molecule. Lacking molecular chirality, the CD spectrum of crocetin is a zero line (not shown).

### 2.1. Binding of crocetin to HSA

In the course of investigations of crocetin–albumin interaction increasing amounts of HSA were added to the carotenoid solution keeping its concentration at $1\times10^{-5}$ M while varying the crocetin/albumin molar ratios from 20.2/1 to 1/15.7 (see Section 4). Unfortunately, limited solubility of crocetin did not permit the reversed titration. In agreement with the earlier observations,[13] the visible absorption curve of crocetin is shifted to longer wavelengths in the presence of albumin (Fig. 3). The red shift is practically complete at equimolar crocetin/HSA ratio and the peak positions and band shape are not altered by further albumin addition (Fig. 4).

Human serum albumin does not absorb light at wavelengths above 300 nm, therefore, despite its high degree of chirality, it has no CD activity in the visible region. The crocetin–HSA complex, however, shows definite, opposite CD bands with nearly equal intensities (Fig. 5). Similarly to the absorption band, the negative and positive Cotton effects carry vibrational fine structure with negative maxima at about 470 and 445 nm and a positive one at 402–405 nm (a positive shoulder appears at 426 nm). The band positions correspond to the crocetin visible absorption but does not match exactly the absorption maxima. CD signals were even detected at the highest carotenoid/albumin ratio (1/15.7) used in the titration experiment. CD band shapes and peak positions have not changed during the titration. The observed Cotton effects were most intense when the crocetin–HSA ratio was 1/0.9 and reduced gradually as the albumin concentration increased. However, taking into account the fact that the chiral signal stems from carotenoid–protein complexes and that the albumin concentration was varied in the course of the experiment, maximum CD intensities measured at 403 nm were divided by the corresponding amounts of albumin and plotted against values of the crocetin/HSA molar ratios (Fig. 6). As can be seen the curve has a maximum around the value of 4.2 suggesting that this ratio gives the highest fraction of albumin molecules binding crocetin molecules which are responsible for the exciton signal. Upon further addition of albumin to the sample, the CD intensity increases, although it lags behind the increase in albumin concentration. This finding is in full

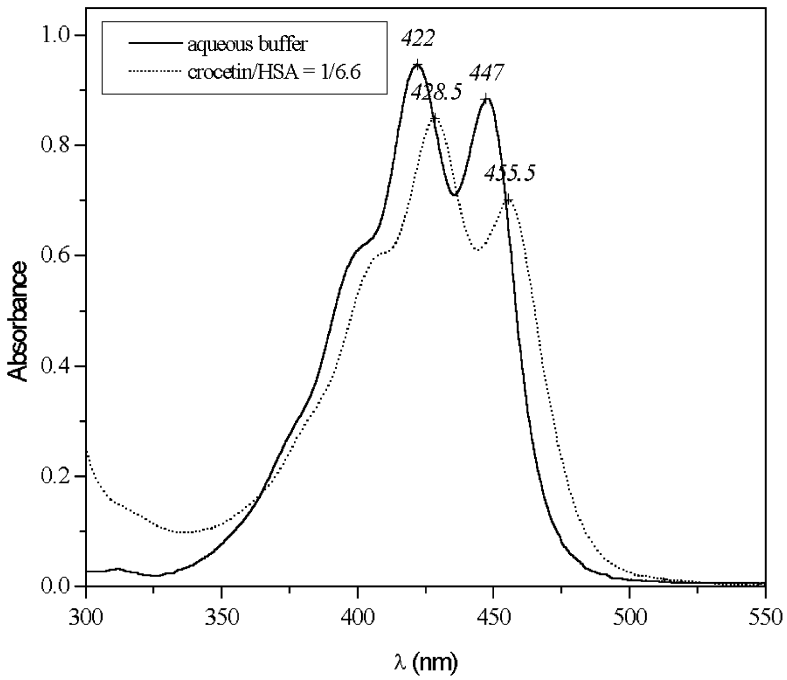


**Figure 3.** UV–vis spectra of crocetin in the presence and absence of HSA.

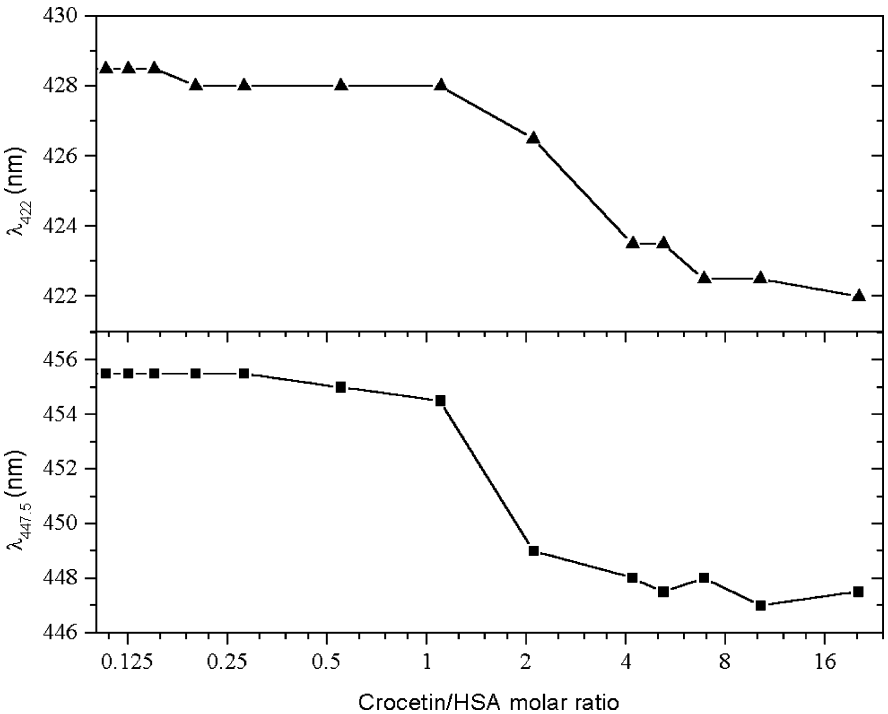


**Figure 4.** The changes of the absorption peak positions of crocetin upon binding to HSA.

harmony with the results obtained from the absorption spectral data. The albumin-bound fractions of crocetin was calculated at the different protein concentrations (see Section 4) and was used to express the average values of the bound crocetin molecules/albumin reaching its maximum—1.6 crocetin molecule/albumin—at 4.2 ligand/protein ratio. Fig. 6 shows that the two curves obtained from different experimental data and treatment are in excellent agreement.

### 2.2. CD/UV–vis titration of 1:1 crocetin–HSA complex with palmitic acid

Fig. 7 shows the effect of palmitic acid addition on the CD and absorption spectra of crocetin–HSA complex. The increase in fatty acid concentration reduces both positive and negative CD bands and shifts the visible absorption spectrum to shorter wavelengths indicating the displacement of crocetin molecules from HSA.

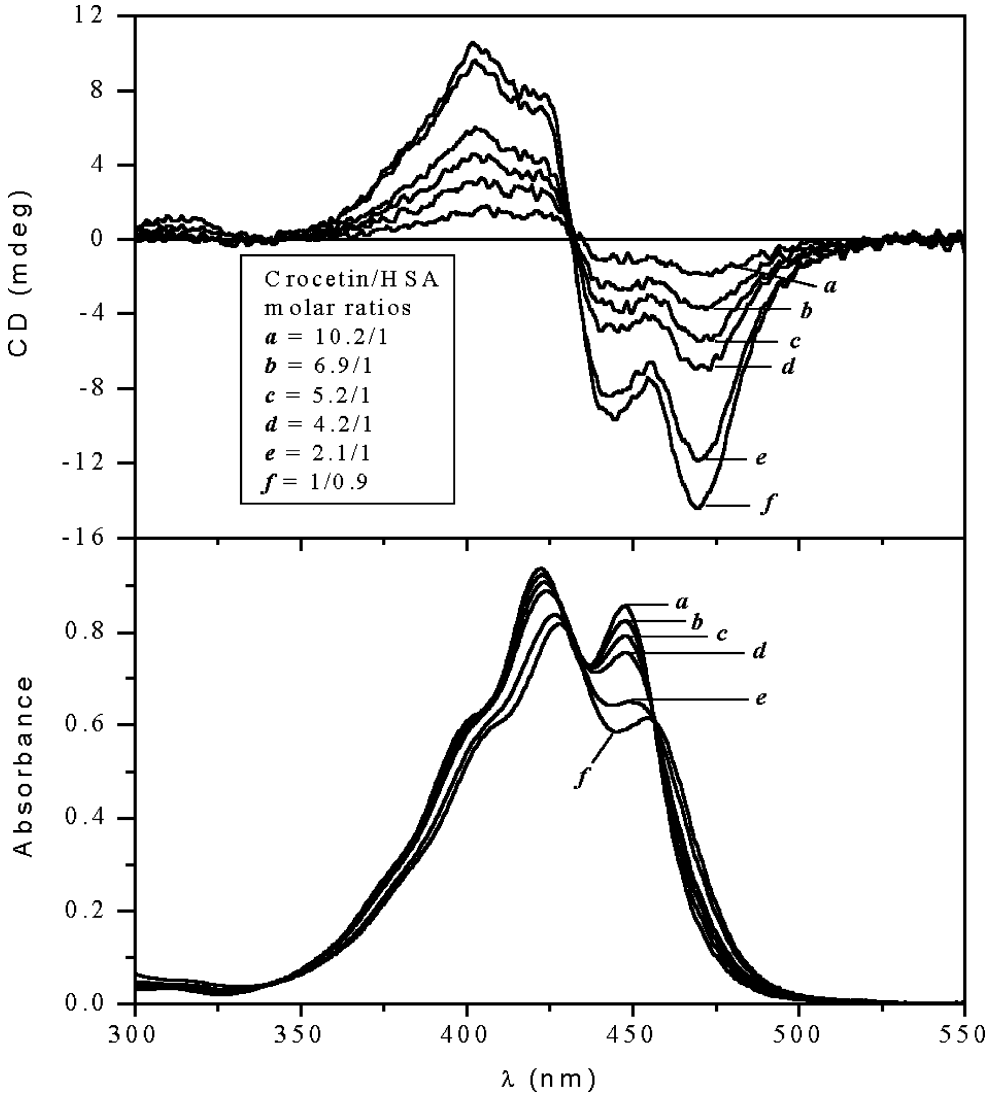


**Figure 5.** Circular dichroism and UV–vis spectra of crocetin bound to HSA. The concentration of crocetin was constant ($10^{-5}$ M). HSA was added as aliquots of a stock solution. Selected spectra are shown at different crocetin–HSA molar ratios.

### 2.3. Fitting of crocetin molecules to the long-chain fatty acid binding sites of HSA

In agreement with the earlier observation,[13] our CD titration experiment also suggests the binding of crocetin to the fatty acid sites of HSA. As numerous biochemical studies proved, fatty acids have multiple binding sites on albumin but, until recently, there were no exact data available on their nature and localization. Fortunately, in the last years precise X-ray crystallographic studies have been published identifying and featuring distinct binding sites of HSA occupied by medium-chain and long-chain fatty acids. Focusing the latter (C16 palmitic and C18 stearic acids), the most important conclusions are briefly summarized:[27]

(i) The high-resolution structures revealed seven, asymmetrically distributed sites on HSA which bind long-chain fatty acids (Fig. 8a).

(ii) Site 1 corresponds to a D-shaped cavity of subdomain IB. Site 2 featured with considerably enclosed binding environment lying between subdomains IA and IIA. In subdomain IIIA, a pair of long-chain fatty acid molecules occupies sites 3 and 4 approximately in a T-shape formation. As a hydrophobic channel, site 5 spans the width of subdomain IIIB binding a single fatty acid molecule in an extended linear conformation. Site 6 located on the outer portions of the protein with contribution of subdomains IIA and IIIA, respectively. Within subdomain IIA, site 7 (suggested to be a primary binding site for shorter-chain fatty acids) binds long-chain fatty acids in a curved configuration.

(iii) At all sites, except for 6 and 7 which have been suggested to have low affinity toward long-chain fatty acids, the carboxylate groups are involved in definite electrostatic interactions with basic and polar side-chains of amino acids.

(iv) Highest affinity binding sites were suggested to belong to the set of sites 1–5. Among them, at least one is located in domain I (site 2) and in domain III, respectively.

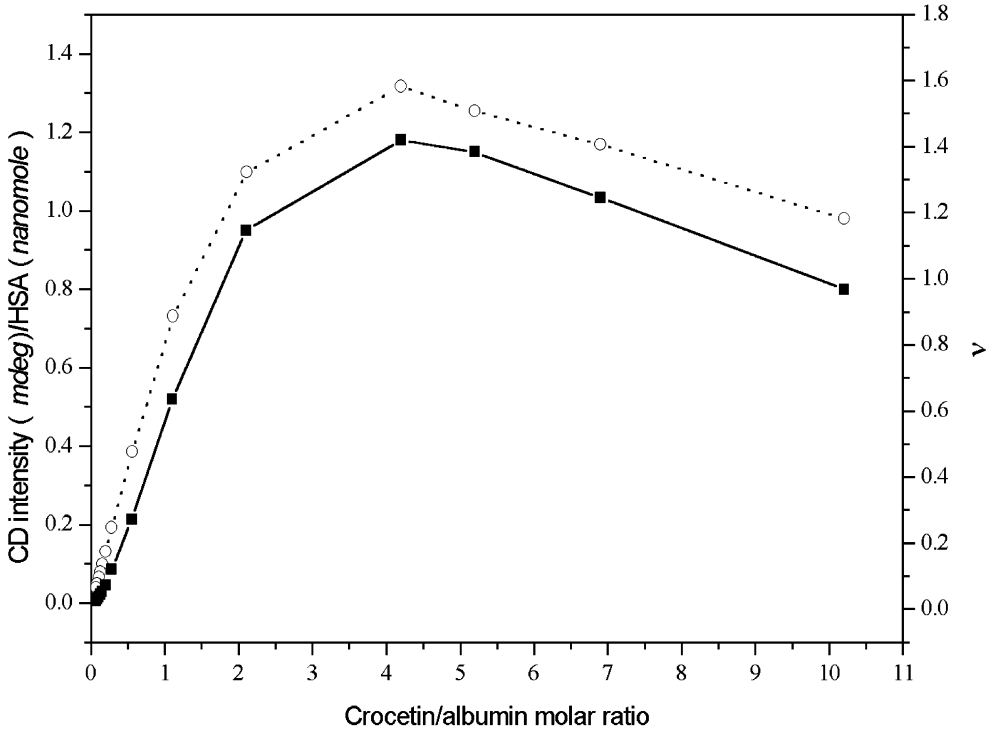


**Figure 6.** —■— (left axis): Plot of the CD intensities (mdeg) at 403 nm divided by the corresponding amounts of HSA (nanomole) against the crocetin/HSA molar ratios. —○— (right axis): Plot of the average values of mole of bound crocetin/albumin.

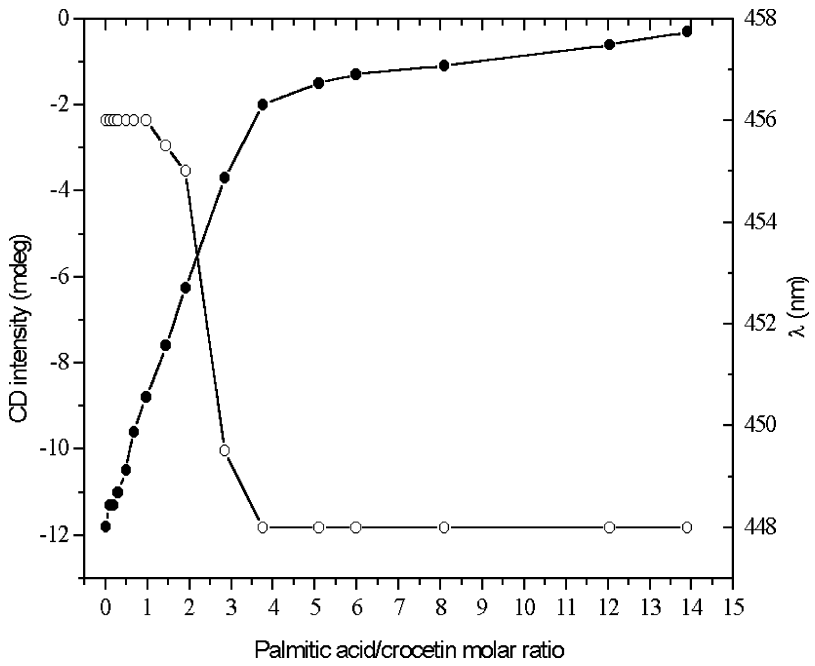


**Figure 7.** Effect of the palmitic acid addition on the CD and visible absorption spectra of crocetin–HSA (1:1) complex. —●— represents the CD intensity measured at 470 nm; —○— shows the longest wavelength absorption peak position in nm.

Taking into consideration its molecular dimensions, palmitic acid is the most similar to crocetin, therefore, the X-ray crystal structure of HSA–palmitic acid complex (Fig. 8a) was used to perform molecular modeling operations fitting six carotenoid molecules to the long-chain fatty acid binding sites of 1–6 (Fig. 8b). Since the explicit position and electrostatic interactions of the long-chain fatty acid carboxylate groups at site 7 could not be determined,[27] it was excluded from this operation (on Fig. 8a and b the palmitic acid bound at site 7 was left in its original location). Consistent with the crystallographic results, carboxylate groups of the cro-

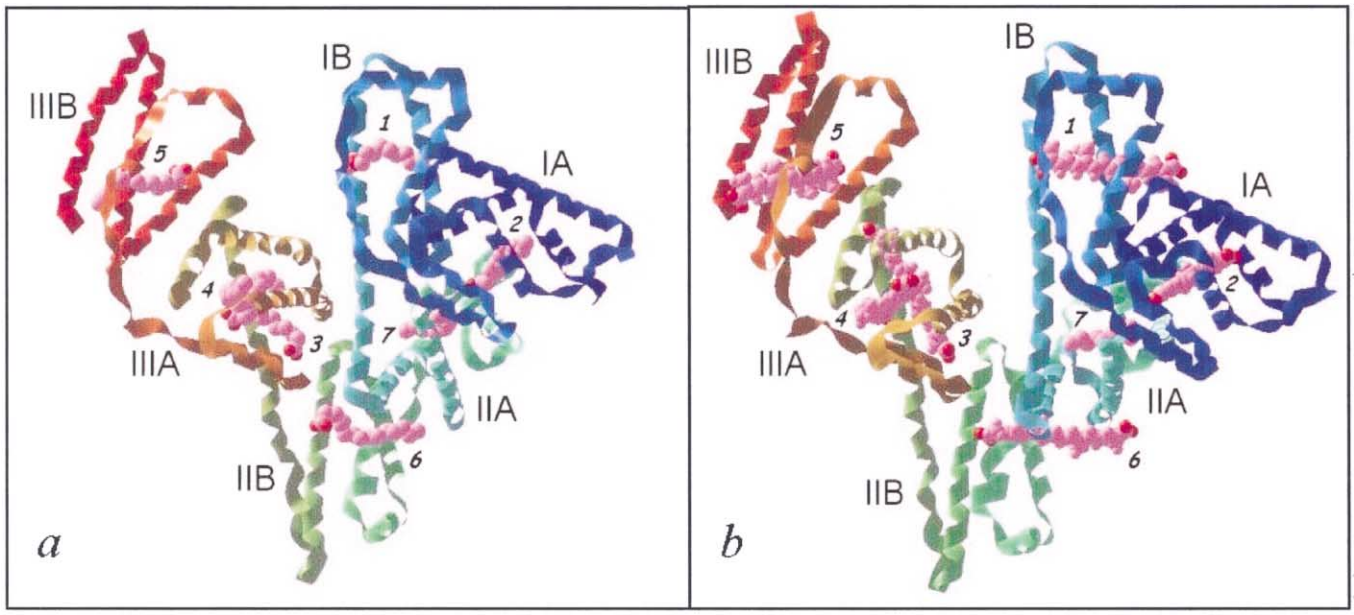


**Figure 8.** X-Ray crystallographic structure of HSA complexed with seven palmitic acids (PDB ID code: 1e7h). The ligand molecules are shown in a space-filling representation and are colored by atom type (carbon, pink; oxygen, red). (b) Structure of the crocetin–HSA complex resulted by fitting of six crocetin molecules to the long-chain fatty acid binding sites 1–6 (the site 7 palmitic acid is in its original position; see text).

cetins were found within hydrogen bonding distances with amino acid residues.

It is worth mentioning that both carboxylate groups of crocetin in site 4 were found to be involved in hydrogen bonding, suggesting extra stabilization factors for crocetin binding at this site (Fig. 9). Crystallographic analysis of palmitic acid–HSA and stearic acid–HSA complexes suggested that only fatty acids containing at least 18 carbon atoms are able to bridge the distance between the polar ends of the site 4 pocket. Including its carboxylate groups, the crocetin backbone is composed only of 16 carbon atoms, but the conjugated double bonds make it a rigid, stick-like molecule showing minimal conformational mobility.

In contrast to this, saturated fatty acids, having single C–C bonds, may readily adopt several conformations, it is not surprising, therefore, that their chains are not fully extended in the hydrophobic channel of site 4 (Fig. 8a) as quantified by the distances between their terminal carbon atoms (16 Å for palmitic acid and 18.2 Å for stearic acid, respectively). On the other hand, for crocetin bound at site 4, this value is 18.7 Å confirming its ability to participate in hydrogen bonding simultaneously at both ends (Fig. 9). Furthermore, it should be noted that only subdomain IIIA contains such binding sites which hold their potential ligands in close proximity (within 15 Å).

X-Ray crystallographic analysis of the HSA–myristate complex suggested that within the IIIA pocket fatty acids may bind cooperatively.[25] This observation is in accordance with an earlier binding experiment performed on BSA in which C16 dicarboxylic fatty acids were found to bind cooperatively to domain III.[34]

## 3. Discussion

It is well known from a large body of spectroscopic studies that albumin may serve as a chiral template for optically inactive compounds producing induced CD bands according to the absorption region of ligands.[18] Among these examples, bilirubin–albumin binding is one of the most studied cases when intense, bisignate, exciton-coupled CD bands reveal how protein binding results in a chiral conformation.[35] Analogously, the CD spectrum appearing upon binding of crocetin to HSA is very characteristic of a chiral exciton splitting between the polyene chromophores. It is important to note, however, that for bilirubin, the excitonic interaction takes place between the covalently linked dipyrrinone chromophores (intramolecular exciton coupling). Binding of a single crocetin molecule to HSA would produce only a monosignate, presumably weak CD band in the visible region, associated with the $\pi \rightarrow \pi^*$ excitation of the conjugated bonds perturbed by the stereogenic centers of the amino acids. Additionally, *cis–trans* isomerization of the polyene chain as a source of the observed CD bands can also be excluded. Thus, the experimentally found CD spectrum refers to an exciton system in which *intermolecular exciton coupling* arises between at least two crocetin molecules bound to HSA. Vibrational fine structure of the CD bands indicates that the vibronic components split individually. Experimental CD and UV–vis spectra of the equimolar crocetin–HSA solution were resolved to Gaussian components to demonstrate how these splittings occur (Fig. 10). The Gaussian analysis of the main absorption band shows four components centered at 457.5, 428, 402.5 and 375 nm corresponding to the 0-0, 0-1, 0-2 and 0-3 vibronic transitions, respectively.

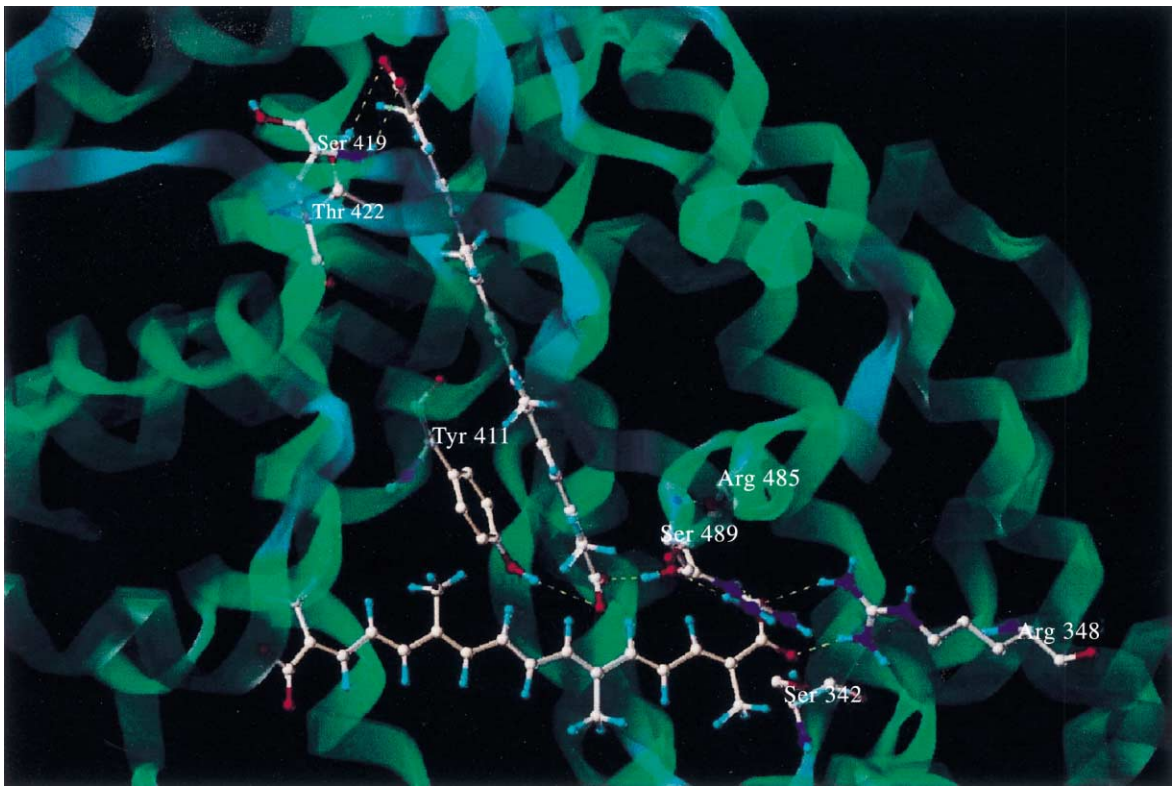


**Figure 9.** Crocetin molecules fitted to sites 3 and 4 in sub-domain IIIA. Carboxylate group of site 3 crocetin is in hydrogen bonding distance to Ser342 and Arg348 from IIB subdomain. At one end, site 4 ligand carboxylate group is in suitable position for hydrogen bonding by Tyr411 and Ser489 and at the other end by Ser419 and Thr422 (these amino acids belong to subdomain IIIA). Carotenoid molecules are shown as ball-and-stick models. Ligand and side chain atoms and bonds are colored by atom type (C, gray; O, red; N, blue; H, light blue).

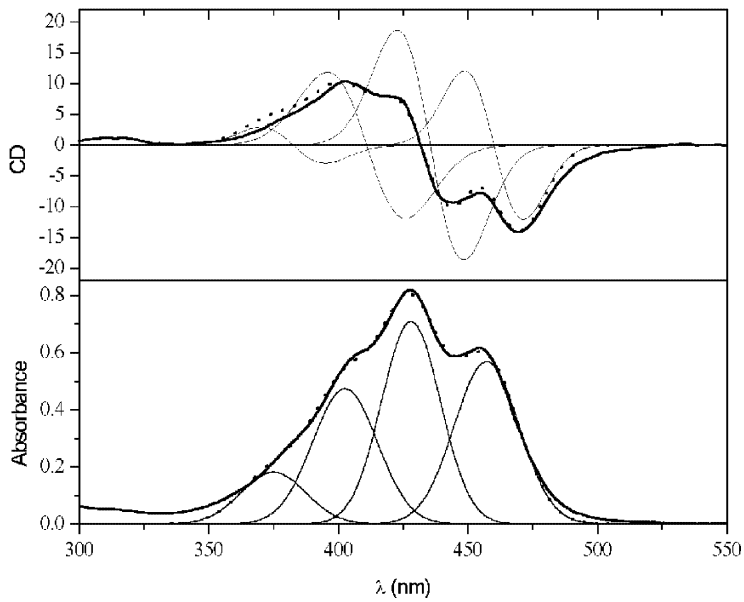


**Figure 10.** Gaussian subband analysis of the CD and visible absorption spectra of crocetin–HSA solution (molar ratio is 1/0.9). [—] experimental spectrum; [- - - -] simulated spectrum; [—] deconvoluted Gaussian components (simulation of the CD and UV–vis absorption curves of crocetin–HSA solution (1/0.9) were performed by nonlinear regression analysis applying four Gaussian functions fitted to the experimental spectra).

Accordingly, there are four Gaussian CD couplets each of which having minus-plus order of the sign from the longer wavelength side leading of their coalescence to the CD curve measured experimentally.

Palmitic acid competes with crocetin for common binding sites of HSA in agreement with Ref. 13 and reduce the induced CD intensities. In Fig. 7 the negative CD extrema measured at 470 nm and the position of the longest wavelength visible absorption peak were plotted together against palmitic acid/crocetin molar ratios. Between 0.1/1 and 2/1 ratios there is only a minor wavelength shift (456→455 nm), while the CD values decrease approximately by half (−11.3→−6.25 mdeg). This suggests, on the one hand that in the above range the majority of crocetin molecules are bound to HSA and only a small fraction is displaced by the fatty acid. On the other hand, it seems that this displacement involves just the site(s) which play a decisive role in the excitonic interaction while crocetin bound at other sites are excitonically 'silent'. Furthermore, of note that the positive CD band becomes unmeasurable when the palmitic acid/crocetin ratio is $\geq 2.85$, but a weak negative band still persists (Fig. 7) presumably due to the chiral perturbation of a single crocetin bound in the chiral protein environment.

Amplitudes of excitonic Cotton effects are inversely proportional to the square of the interchromophoric distance and proportional to the square of the extinction coefficients.[36,37] Furthermore, the amplitude is also dependent on the angle between the electric transition dipoles of the interacting chromophores. There is no coupling, if this angle is 0 or 180°, whereas coupling is maximal at an angle of ca. 70°.[36] According to the exciton chirality rule,[36,37] the signed order of the bisignate Cotton effects can be utilized to assign the relative orientation of the electronic transition moments (oriented along the long axis of the polyene chromophore). The observed sign order, a negative CE at long wavelength followed by a positive one at shorter wavelength, corresponds to the case termed by negative or left-handed chirality. Stereochemically, this means that there is a negative angle between the coupled transition dipoles. Therefore, it is reasonable to examine the molecular model of HSA fitted with six crocetin molecules in order to find correlation between experimental and computational results. On the basis of our molecular model, Fig. 11 shows some examples to illustrate left-handed and right-handed geometrical positions of fitted molecules of crocetin leading to negative and positive chirality, respectively. Table 1 summarizes all intermolecular angles and distances measured between crocetin molecules fitted to the long-

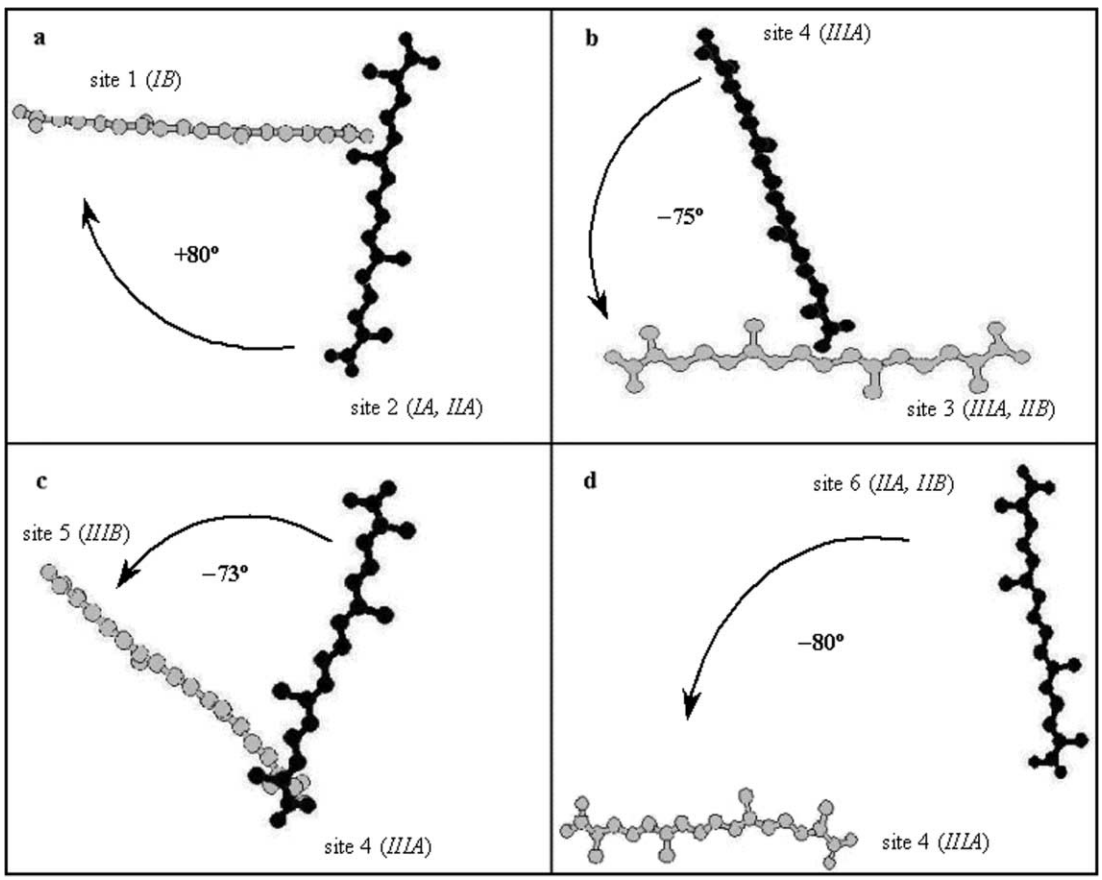


**Figure 11.** Pictorial representation of right (a) and left-handed (b,c,d) geometrical arrangements of crocetin molecules fitted to the long-chain fatty acid binding sites of HSA (drawn on the basis of the molecular model showed in Fig. 8b). In the case of a, the longer wavelength Cotton effect should be a positive; b, c and d give the sign order found experimentally. For intermolecular distances see Table 1.

**Table 1.** Intermolecular angles (expressed in degrees) and distances [in Å] measured between the six crocetin molecules fitted to the long-chain fatty acid binding sites of HSA (intermolecular spacings were taken between the geometrical centers of the molecules)

| | Site 1 | Site 2 | Site 3 | Site 4 | Site 5 |
|---|---|---|---|---|---|
| Site 2 | +80 [20] | – | – | – | – |
| Site 3 | +55 [34] | +84 [40] | – | – | – |
| Site 4 | −83 [34] | ~0 [40] | −75 [11] | – | – |
| Site 5 | +150 [42] | −80 [55] | −107 [25] | −73 [20] | – |
| Site 6 | ~0 [37] | +114 [30] | −120 [27] | −80 [30] | −140 [50] |

chain fatty acid binding sites 1–6. Combinations with a positive angle should give right-handed chirality and can therefore be neglected (sites 1–2, 1–3, 1–5, 2–3 and 2–6). Additionally, zero angle gives no excitonic CD bands (sites 1–6 and 2–4). Although the carotenoid polyene chain is exceptionally strong chromophore, developing measurable excitonic splitting is unrealistic at intermolecular distances of about 30 Å or more. Furthermore, site 6, exposing its ligand to the polar environment, was stated to be low affinity toward long-chain fatty acids.[27] Finally, we have only three suitable combinations (sites 3–4, 3–5 and 4–5) which may be responsible for the induced CD spectrum. All of them are located on domain III, which is thought to contain high affinity binding sites for long-chain fatty acids. Most probably, the chiral exciton signals may stem from the interaction of crocetin molecules bound at sites 3–4 and/or sites 4–5.

The measure of chirality is the so called $g$ or anisotropy factor defined as $\Delta A/A$ where $\Delta A$ is the difference in absorption of the left and right circularly polarized light ($A_l$–$A_r$) and $A$ is the sample absorption. $\Delta A$ values can be obtained from the CD spectra measured in millidegrees according to the equation of $\Delta A = 4\pi\Theta$ (degrees)/180ln10. Plotting absolute values of $g$ calculated at 470 nm against the crocetin/HSA molar ratios (Fig. 12) shows that the maximum value ($1.3\times10^{-3}$) belongs to the equimolar solution (1/0.9) because it has the largest absolute amount of albumin molecules binding two carotenoids in a left-handed geometry. In order to the comparability, CD data are commonly expressed in molar units i.e. $\Delta\varepsilon$, which can be obtained from $\Delta A/cl$, where $c$ is the concentration of the optically active compound in mol/dm$^3$ and $l$ is the optical pathlength in cm. In our case, however, only the total concentration of crocetin is known ($10^{-5}$ M), but not of the part of bound fraction being responsible for the excitonic CD activity. Trying to get an approximate value for it, an important property of fatty acid binding can be utilized. As was demonstrated by Spector and Fletcher,[15] in oleate–HSA solution with 1/1 molar ratio, 31% of the albumin molecules have no oleate, 43% binds 1, 22% 2 and 4% 3 oleates, respectively. Obviously, multiple binding sites with different affinities (association constants are ranged from $11.8\times10^7$ to $5.5\times10^7$ M$^{-1}$ for 4 binding sites) result in this dynamic, complex equilibrium. As a first approximation, we assumed that a similar distribution exists in the 1/0.9 crocetin/HSA solution (this solution contains $2\times10^{-8}$

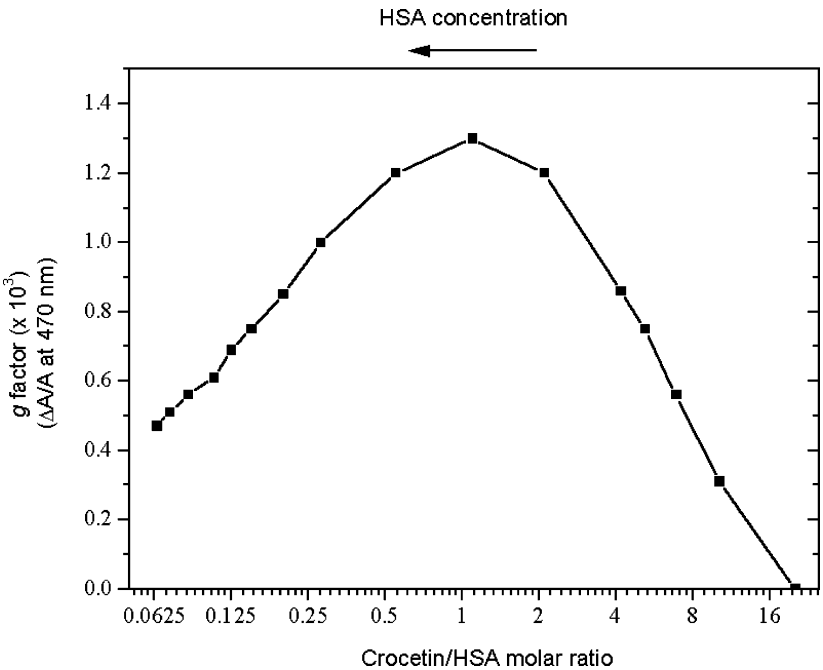


**Figure 12.** Absolute values of the $g$ factor calculated at 470 nm plotted against the crocetin/HSA molar ratios.

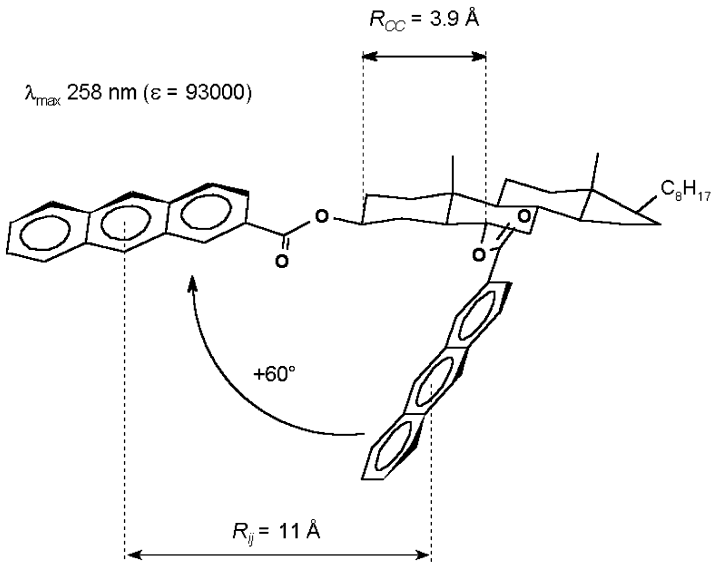


**Figure 13.** Right-handed intramolecular exciton coupling of 5-cholestane-3β,6α-bis-(2-anthroate). Redrawn from Ref. 38.

mol albumin and $2.13\times10^{-8}$ mol crocetin). Assuming that 25% of the $2\times10^{-8}$ mol albumin binds two crocetin molecules, the concentration of the complex which gives rise to excitonic CD bands is $2.3\times10^{-6}$ mol/dm$^3$ (sample volume is 2.13 mL). Using this value to calculate molar CD intensities we obtain +136 $\Delta\varepsilon$ at 401.5 nm and −186 $\Delta\varepsilon$ at 470 nm (for $10^{-5}$ M crocetin concentration the calculation gives +32 and −44 $\Delta\varepsilon$ values, respectively). This result was compared with a model compound, a very rigid steroidal skeleton substituted with two anthroate moieties having very similar molar extinction coefficient to crocetin (Fig. 13). The exciton splitting between the anthroate chromophores held in a right-handed position gives rise to a typical positive–negative couplet (+240 and −240 $\Delta\varepsilon$) in the 250–280 nm region.[38] Thus, the above estimation seems to be concordant with the notion that since more than two potential binding sites exist, within the 25% fraction probably not every albumin molecule binds from their two ligands in a suitable position for the chiral exciton coupling.

The red shift of the visible absorption spectrum also results from this intimate carotenoid–protein interaction. In general, four mechanisms may cause absorption spectral shifts. Rhodopsin is a well known example for the charge-induced energy shift.[39] The second type are the spectral changes due to excitonic interactions.[36,37] The third one is the shift induced by dispersion interactions. Finally, conformational variations may also modify the electronic excitation energy. The first mechanism cannot be invoked for the observed small excitation energy lowering. As the CD spectrum proves, there is a chiral exciton coupling between the bound polyene chromophores which might have an effect on the absorption band either. However, according to the molecular exciton model, a red shift occurs only if the absolute value of the angle between the coupled electronic transition moments is larger than 90°. Crocetin pairs in sites 3–4 and 4–5, do not fulfill this condition (see Table 1). Furthermore, if the crocetin–crocetin excitonic interaction would be responsible for both CD and absorption spectral changes then the visible band should be blue shifted (back to its original position measured in the absence of albumin) parallel with the decreasing crocetin/HSA ratio. The CD band amplitudes decrease (Fig. 4) because the HSA excess shifts the equilibrium to the 1 crocetin molecule/HSA complex having no excitonic CD activity. Contrary to this, the red-shifted visible absorption band does not show significant changes from 1/0.9 to 1/15.7 ligand/HSA ratio. It can be concluded, therefore, that the bathochromic shift has no excitonic contribution.

It is well established, that the polyene absorption spectrum is shifted to lower energy as the solvent polarizability increases.[40] Fatty acid binding pockets on albumin are featured with strongly apolar environment. When crocetin binds to the protein, the low polarizability medium (water) is exchanged by the high polarizability protein surroundings which promotes the induced dipole–induced dipole interactions (dispersion forces) causing the bathochromic shift.[41] Taken together, dispersion interactions seem to be responsible for the decrease in the excitation energy of the $^1A_g \rightarrow {}^1B_u$ transition.

## 4. Experimental

### 4.1. Materials

Essentially fatty acid free HSA, palmitic acid and crocetin (pyridine salt, 95% purity grade) were purchased from Sigma Co., and used as supplied. Double distilled water and HPLC grade ethanol (Chemolab, Hungary) were used. All other chemicals were analytical grade.

### 4.2. Absorbance and CD measurements

CD and ultraviolet–visible (UV–vis) spectra were recorded on a Jasco J-715 spectropolarimeter at 25± 0.2°C in a rectangular cuvette with 1 cm pathlength. Temperature control was provided by a Peltier thermostat equipped with magnetic stirring. The spectra were accumulated three times with a bandwidth of 1.0 nm and a resolution of 0.5 nm at a scan speed of 100 nm/min.

In order to avoid molecular aggregation, crocetin was dissolved in a 0.2 M borate/boric acid buffer (pH 8.5) at $1\times10^{-5}$ M. To keep the crocetin concentration constant during spectrophotometric titration, this solution was used to prepare the HSA stock solution ($5\times10^{-4}$ M).

**4.2.1. CD/UV–vis titration of crocetin with HSA**. A 1 cm cuvette was filled with crocetin solution ($1\times10^{-5}$ M, 2 mL). After recording the CD and absorbance spectra between 205–550 nm, a volume of HSA solution ($5\times10^{-5}$ M, 20 μL) was added and the spectra were taken from 240 to 550 nm under mild magnetic stirring. This procedure was performed five times to obtain spectra at 20.2/1, 10.2/1, 6.9/1, 5.2/1 and 4.2/1 crocetin/HSA molar ratios. To decrease further this ratio, 10, 20, 40, 80, 80, 80, 80, 160, 160 and 160 μl of $5\times10^{-4}$ M HSA solution was added consecutively to achieve 2.11/1, 1/0.9, 1/1.8, 1/3.55, 1/5.1, 1/6.6, 1/8, 1/9.3, 1/11.7, 1/13.8 and 1/15.7 crocetin/HSA molar ratios respectively. The spectra showed no time dependence.

**4.2.2. CD/UV–vis titration of crocetin–HSA (1:1) complex by palmitic acid**. In a 1 cm pathlength cell HSA solution ($5\times10^{-4}$ M, 40 μL) was added to crocetin solution ($1\times10^{-5}$ M, 2 mL) to obtain 1:1 molar ratio. After measuring the CD/UV–vis spectra between 240–550 nm, μL volumes of palmitic acid solutions (10, 10 and 10 μL from $2\times10^{-4}$ M solution, 10, 10 and 15 μL from $4\times10^{-4}$ M solution and 10, 10, 20, 20, 30, 20, 50, 100 and 50 μL from $1\times10^{-3}$ M solution) were added to achieve the required ratios (from 0.1/1 palmitic acid/crocetin molar ratio to 14/1). Palmitic acid solutions were prepared with ethanol containing $1\times10^{-5}$ M crocetin.

### 4.3. Calculation of the albumin-bound fraction of crocetin

The visible absorption spectra measured at different crocetin/HSA molar ratios were reconstructed by the combination of the absorption spectra obtained in a buffer solution (100% unbound species, see Fig. 2) and in the presence of the highest albumin concentration (100% bound species, $c_{HSA}=160$ μM) using a nonlinear regression analysis. The corresponding numerical factors found in each case (not shown) were used to calculate the protein-bound part of crocetin.

### 4.4. Molecular modeling calculations

All computer modeling procedures were carried out using the Sybyl 6.6 program (Tripos Inc., St. Louis, MO) on a Silicon Graphics Octane workstation under Irix 6.5 operation system. The three-dimensional coordinates of HSA complexed with palmitic acids were obtained from the Protein Data Bank (entry PDB code 1e7h[27]).

First, six molecules of palmitic acid bound to sites 1–6 were replaced by crocetin molecules using the multifit command.

The resulting complex was then energy-minimized with the Powell Conjugate Gradient method applying Tripos Force Field until the convergence was less than 0.01 kcal/(molÅ).

## Acknowledgements

The authors gratefully acknowledge helpful discussions with Dr. Ilona Fitos (Department of Molecular Pharmacology). This work was supported by grants from the Hungarian National Scientific Fund (OTKA T 030271 and T 033109).

## References

1. Nair, S. C.; Kurumboor, S. K.; Hasegawa, J. H. *Cancer Biother*. **1995**, *10*, 257–264.
2. Ríos, J. L.; Recio, M. C.; Giner, R. M.; Mánez, S. *Phytother. Res*. **1998**, *10*, 189–193.
3. Pfander, H. *Key to Carotenoids*; Birkhäuser: Basel, 1987; p. 209.
4. Jagadeeswaran, R.; Thirunavukkarasu, C.; Gunasekaran, P.; Ramamurty, N.; Sakthisekaran, D. *Fitoterapia* **2000**, *71*, 395–399.
5. Abdullaev, F. I. *Toxicol. Lett*. **1994**, *70*, 243–251.
6. Wang, C. J.; Lee, M. J.; Chang, M. C.; Lin, J. K. *Carcinogenesis* **1995**, *16*, 187–191.
7. Holloway, G. M.; Gainer, J. L. *J. Appl. Physiol*. **1988**, *65*, 683–686.
8. Gainer, J. L.; Rudolph, D. B.; Caraway, D. L. *Circ. Shock* **1993**, *41*, 1–7.
9. Singer, M.; Stidwill, R. P.; Nathan, A.; Gainer, J. L. *Crit. Care. Med*. **2000**, *28*, 1968–1972.
10. Gainer, J. L.; Jones, J. R. *Experientia* **1975**, *31*, 548–549.
11. Gainer, J. L.; Chisolm, G. M. *Atherosclerosis* **1974**, *19*, 135–138.
12. Chisolm, G. M.; Gainer, J. L.; Stoner, G. E.; Gainer, J. V. *Atherosclerosis* **1972**, *15*, 327–343.
13. Miller, T. L.; Willett, S. L.; Moss, M. E.; Miller, J.; Belinka, B. A. *J. Pharm. Sci*. **1982**, *71*, 173–177.
14. Carter, D. C.; Ho, J. X. *Adv. Protein. Chem*. **1994**, *45*, 153–203.
15. Peters, T. *All About Albumin*: *Biochemistry*, *Genetics and Medical Applications*; Academic Press: San Diego, 1996; pp. 55–83.
16. He, X. M.; Carter, D. C. *Nature* **1992**, *358*, 209–215.
17. Sugio, S.; Kashima, A.; Mochizuki, S.; Noda, M.; Kobayashi, K. *Protein Eng*. **1999**, *12*, 439–446.
18. Dockal, M.; Carter, D. C.; Rüker, F. *J. Biol. Chem*. **1999**, *274*, 29303–29310.
19. Spector, A. A. *J. Lipid Res*. **1986**, *16*, 165–179.
20. Hamilton, J. A. *J. Lipid Res*. **1998**, *39*, 467–481.

21. Cistola, D. P.; Small, D. M.; Hamilton, J. A. *J. Biol. Chem*. **1987**, *262*, 10971–10979.
22. Cistola, D. P.; Small, D. M.; Hamilton, J. A. *J. Biol. Chem*. **1987**, *262*, 10980–10985.
23. Hamilton, J. A.; Era, S. E.; Bhamidipati, S. P.; Reed, R. G. *Proc. Natl. Acad. Sci*. **1991**, *88*, 2051–2054.
24. Richieri, G. V.; Anel, A.; Kleinfeld, A. M. *Biochemistry* **1993**, *32*, 7574–7580.
25. Curry, S.; Mandelkow, H.; Brick, P.; Franks, N. *Nat. Struct. Biol*. **1998**, *5*, 827–835.
26. Curry, S.; Brick, P.; Franks, N. P. *Biochim. Biophys. Acta* **1999**, *1441*, 131–140.
27. Bhattacharya, A. A.; Grune, T.; Curry, S. *J. Mol. Biol*. **2000**, *303*, 721–732.
28. Sklar, L. A.; Hudson, B. S.; Simoni, R. D. *Proc. Natl. Acad. Sci*. **1975**, *72*, 1649–1653.
29. Sklar, L. A.; Hudson, B. S.; Simoni, R. D. *Biochemistry* **1977**, *16*, 5100–5108.
30. Reed, R. G. *J. Biol. Chem*. **1986**, *261*, 15619–15624.
31. Berde, C. B.; Hudson, B. S.; Simoni, R. D.; Sklar, L. A. *J. Biol. Chem*. **1979**, *254*, 391–400.
32. Tarantilis, P. A.; Polissiou, M.; Mentzafos, D.; Terzis, A.; Manfait, M. *J. Chem. Crystallogr*. **1994**, *24*, 739–742.
33. Kohler, B. E. In *Carotenoids, Spectroscopy*; Britton, G.; Liaaen-Jensen, S.; Pfander, H., Eds. Electronic structure of carotenoids; Birkhäuser: Basel, 1995; Vol. 1B, pp. 1–12.
34. Tonsgard, J. H.; Meredith, S. C. *Biochem. J*. **1991**, *276*, 569–575.
35. Trull, F. R.; Person, R. V.; Lightner, D. A. *J. Chem. Soc., Perkin Trans. 2* **1997**, 1241–1250.
36. Harada, N.; Nakanishi, K. *Circular Dichroic Spectroscopy—Exciton Coupling in Organic Stereochemistry*; University Science Books: Mill Valley, CA, 1983.
37. Lightner, D. A.; Gurst, J. E. *Organic Conformational Analysis and Stereochemistry from Circular Dichroism Spectroscopy*; John Wiley: New York, 2000; pp. 423–456.
38. Dong, J. G.; Wada, A.; Takakuwa, T.; Nakanishi, K.; Berova, N. *J. Am. Chem. Soc*. **1997**, *119*, 12024–12025.
39. Rando, R. R. *Chem. Biol*. **1996**, *3*, 255–262.
40. Kuki, M.; Nagae, H.; Cogdell, R. J.; Shimada, K.; Koyama, Y. *Photochem. Photobiol*. **1994**, *59*, 116–124.
41. Jouni, Z. E.; Wells, M. A. *J. Biol. Chem*. **1996**, *271*, 14722–14726.